Anti-Glass patterns and real motion perception: Same or different mechanisms?

Maria Michela Del Viva

Dipartimento di Psicologia, Università di Firenze, Firenze, Italy, & Istituto di Neuroscienze, CNR, Pisa, Italy ✉

Monica Gori

Istituto Italiano di Tecnologia, Genoa, Italy, & Dipartimento di Informatica Sistemistica e Telematica, Genoa, Italy ✉

A sequence of anti-Glass patterns, composed by dot pairs with opposite luminance polarity, elicits a clear perception of motion in the direction of the white dot of the pair. This effect can be reversed by introducing a delay in the presentation of white dots, suggesting a faster processing of light dots as a cause of the motion signal (M. M. Del Viva, M. Gori, & D. C. Burr, 2006). If this hypothesis is correct, anti-Glass patterns should interact with real motion signals. In this study, we compare the motion induced by these stimuli to test whether they are analyzed by the same motion mechanism. We found that motion induced by anti-Glass patterns annuls real motion, when they are presented simultaneously in the same display and moving in opposite directions. By lowering the contrast of one of them, motion toward the stimulus with higher contrast prevails. We also found sub-threshold summation of motion induced by anti-Glass patterns and real motion, when presented simultaneously and moving in the same direction.These findings indicate that anti-Glass patterns and moving stimuli are processed by the same, contrast-dependent motion mechanism and lend further support to the proposed explanation of the effect.

Introduction

Glass patterns (Glass, 1969; Glass & Switkes, 1976) are arrays of randomly positioned dot pairs oriented along global patterns. They carry a powerful sense of global spatial structure, and their properties have been widely investigated (Cardinal & Kiper, 2003; Dakin & Bex, 2001; Kurki, Laurinen, Peromaa, & Saarinen, 2003; Seu & Ferrera, 2001; Wilson & Wilkinson, 1998; Wilson, Wilkinson, & Asaad, 1997). Glass patterns have been shown to activate early visual areas as V1 and V2 (Hegdé & Van Essen, 2000; Movshon, Smith, & Kohnet, 2003; Smith, Bair, & Movshon, 2002) as well as brain regions in the ventral pathway (Tanaka, 1992; Wilkinson et al., 2000).

Displaying a succession of such patterns (dynamic patterns), with dipoles randomly repositioned at each screen refresh, conveys a compelling sense of global motion along the dominant orientation of the patterns, even though the stimulus itself contains no physical motion information (Ross, Badcock, & Hayeset, 2000). The direction of perceived motion is ambiguous because the structure is perfectly symmetrical (see Movie 1). Presence and direction of perceived motion depend on distance of dots within the dipole (Ross et al., 2000). A recent electrophysiological study on monkeys (Krekelberg,

Dannenberg, Hoffmann, Bremmer, & Rosset, 2003) showed that Glass patterns activate brain regions in the dorsal pathway devoted to real and apparent motion processing (Britten & van Wezel, 1998; Duffy & Wurtz, 1991; Krekelberg, Vatakis, & Kourtzi, 2005; Mikami, Newsome, & Wurtz, 1986a; Morroneet al., 2000; Newsome & Pare, 1988; Tanaka, Fukada, & Saito, 1989; Zeki, Watson, & Frackowiak, 1993). Psychophysical results are in agreement with electrophysiology (Ross, 2004), showing that perceived direction and speed of global motion is influenced by the presence of Glass patterns.

A variant of the Glass stimulus is given by "anti-Glass" patterns, using dot pairs of opposite luminance polarity (anti-pairs). These create a weaker sense of global structure than regular Glass patterns, sometimes in a direction orthogonal to the global orientation (Dakin, 1997; Glass & Switkes 1976) and are harder to distinguish from randomly oriented dipoles (Prazdny, 1986). They are able to destroy the apparent global structure of Glass patterns when added to them (Barlow & Olshausen, 2004; Burr & Ross, 2006).
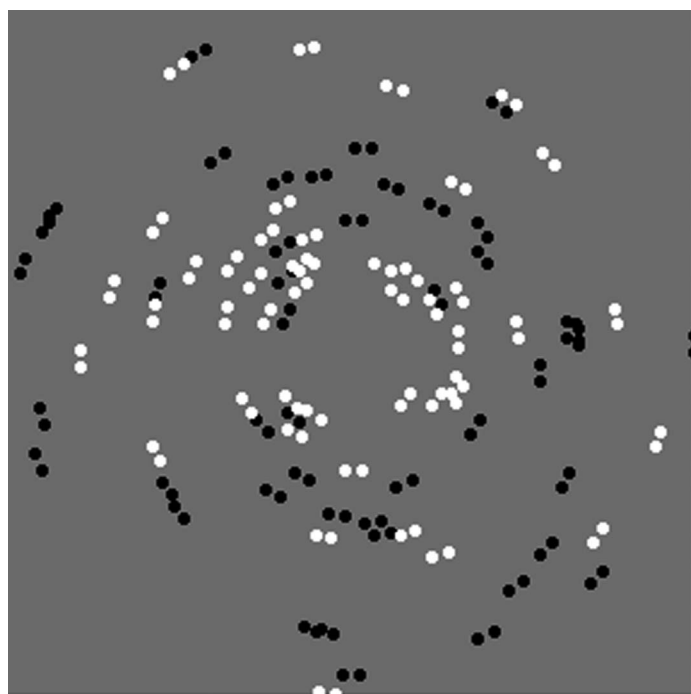
In a previous publication (Del Viva, Gori, & Burr, 2006), it was shown that uncorrelated sequences of anti-Glass patterns produce a clear perception of motion, but unlike the motion caused by Glass patterns, the motion from anti-Glass is always in a specific direction: from the dark to the light dot (see Movie 2). Motion directionality could be

reversed by delaying the presentation of light dots by 5 ms. Control experiments showed that this latency was generated neither by luminance nor contrast asymmetry, like other illusions of contrast induced motion perception (Backus & Oruç, 2006; Conway, Kitaoka, Yazdanbakhsh, Pack, & Livingstone, 2005) nor by biphasic temporal impulse response functions for light increments and decrements (Brooks, van der Zwan, & Holden, 2003). It was therefore hypothesized that the illusory motion could result from a delayed processing of the dark dots due to differential delays in the primate on and off systems, presumably at retinal level (Chichilnisky & Kalmar, 2002; Ueno, Kondo, Niwa, Terasaki, & Miyake, 2004).
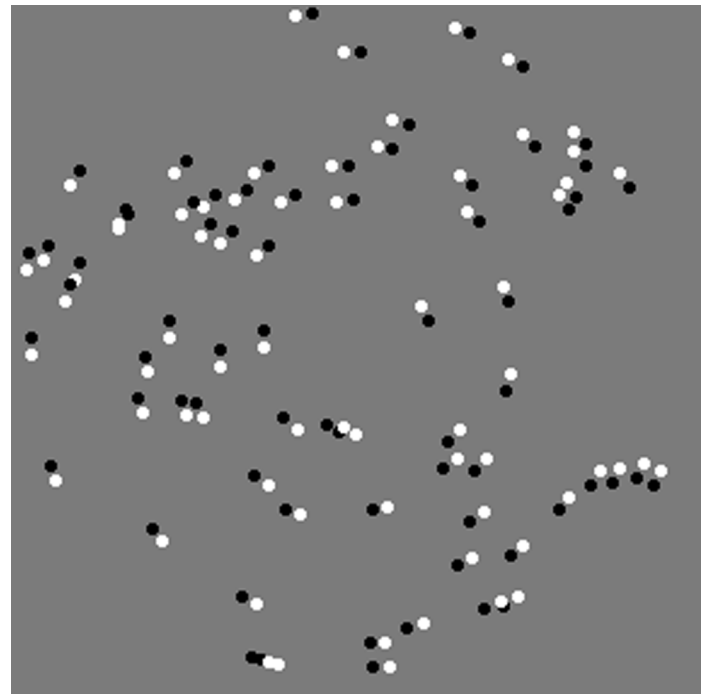
If the above explanation is correct, anti-Glass patterns and real motion should evoke similar activity in direction-selective neurons (such as in V1 cells), implying that anti-Glass should interact with real motion signals.

Current study

In this study, we compared the sensitivity of the human global motion system to anti-Glass patterns and to real optic-flow motion. Since anti-Glass motion is perceived in the direction opposite to time ordering (Del Viva et al., 2006) as in "reverse-phi motion" (Anstis, 1970), we also compared anti-Glass with reversing-contrast moving dots to demonstrate that they are two special cases of the same phenomenon. For this purpose, we devised a rotational optic-flow stimulus, made locally

Movie 2. Motion illusion induced by a sequence of anti-Glass patterns. Motion direction is defined by dot polarity.

of reversing-contrast dots, whose properties have not yet been studied.

We first matched the motion and the anti-Glass stimuli for speed and contrast. Speed matching was obtained by manipulating the distance between dots of anti-Glass pairs and the displacement of moving dots. The time interval was kept constant, according to the assumption that the motion effect of anti-Glass is due to a fixed latency (Del Viva et al., 2006).

Finally, we combined anti-Glass patterns and real motion stimuli in the same display to study the relationship between the processing of the two signals by varying their relative strength. Stimulus strength was adjusted either by varying the proportion of dots of each stimulus or their luminance contrast. The motivation for these two types of manipulations was the suggestion from previous studies that they test different stages of motion analysis: a first contrast-dependent local stage and a second coherence-dependent global stage (Morrone, Burr, & Vaina, 1995). Measuring the contrast sensitivity of the global motion system to the combined stimuli sheds light on the level at which they are integrated.

General methods

Stimuli
Anti-Glass patterns

Stimuli were sequences of circularly arranged anti-Glass patterns, each composed by 70 anti-pairs, made of

Movie 1. Motion illusion induced by a sequence of Glass patterns. Motion direction is ambiguous.

dots with opposite luminance polarity with respect to the background (see Figure 1A and Movie 2). Each pair was randomly positioned within an annulus, delimited by $r_{max} = 13°$ and $r_{min} = 3.5°$, and was oriented tangentially to produce coherent circular patterns. The position of pairs was randomly updated every 6 video frames (30 ms = duration), so that dots were uncorrelated in space and time, providing no motion signals. Five different patterns were displayed in each trial, for a total presentation time of 150 ms.

Motion

Motion stimuli were arrays of 70 random dots that moved coherently along circular trajectories around the screen center. In contrast-reversing stimuli, all dots switched polarity during motion from white to black (see Figure 1C) because white dots are assumed to be processed faster than dark dots (Del Viva et al., 2006). In same-polarity motion stimuli, 50% of the dots were black and 50% were white to match the global luminance of anti-Glass and reverse-phi, and polarity was maintained during motion. Moving dots stayed in a given position for 15 ms before being displaced abruptly, with a total lifetime of 30 ms. After 30-ms dots, position was updated

randomly and total presentation time was 150 ms. As in the anti-Glass stimulus, dots were confined within an annulus delimited by $r_{max} = 13°$ and $r_{min} = 3.5°$.

Apparatus

The background luminance was 61 cd/m^2, maximum luminance was 140 cd/m^2 (white), and minimum luminance was lower than 1 cd/m^2 (black). All stimuli were programmed with Matlab and displayed on a gamma-corrected Clinton Monoray monitor (frame rate 200 Hz, 640 × 480 pixel) via a VSG 2/3 board (Cambridge Research System). The whole display subtended 26° × 26° of visual angle at a viewing distance of 57 cm, and a single dot subtended 0.3° All experiments were carried out in a completely dark room.

Observers

Three observers participated to the experiments, one of the authors (M.G.) and two observers (F.B. and L.B.), naive to the aims of the study. All observers had normal or corrected to normal visual acuity and no history of visual disorders.
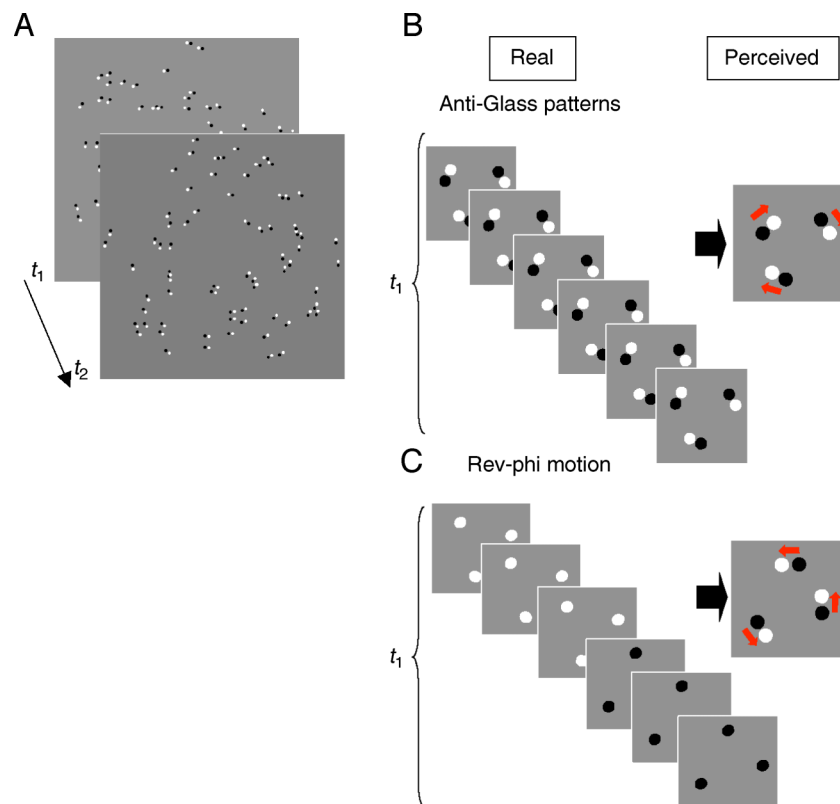

Figure 1. (A) Example of anti-Glass stimuli used in this study. The position of pairs is updated randomly every 6 video frames (t_1 = duration = 30 ms). (B) Schematic representation of the anti-Glass stimulus during time t_1 that corresponds to 6 video frames (frame-rate 200 Hz). Dots are presented simultaneously (left), but the stimulus is perceived as moving in the direction of the white dot (right). (C) Left: schematic representation of the reversing-contrast stimulus during time t_1. Right: motion is perceived in the opposite direction (reverse-phi motion).

Dependence on speed

Stimuli and procedures

In anti-Glass patterns, coherence discrimination thresholds were measured by degrading the circular patterns by replacing a fraction of the 70 pairs with spatially uncorrelated pairs with random orientation (noise). The degree of coherence was kept constant throughout each trial sequence. Relative position of all light and dark dots was randomly assigned on each trial. In motion stimuli, coherence discrimination thresholds were measured by degrading the coherent circular flow by replacing a fraction of the 70 pairs with dots moving in random directions (noise).

For all stimuli, motion direction was randomized between trials, and the proportion of signal and noise pairs was varied from trial to trial according to a QUEST staircase procedure (Watson & Pelli, 1983). The subject's task was to indicate the direction of perceived motion, in a two-alternative forced-choice procedure (2AFC) with a single temporal presentation.

Thresholds for moving stimuli were measured for displacements (center to center) from $0.05°$ to $1°$, while for anti-Glass the lowest distance was $0.4°$, corresponding to a two-pixel separation between dot boundaries. Note that since dot separation was the same for all pairs, local angular rotation speed decreased with the inverse of the distance from the center of the screen. While these stimuli did not exactly simulate real global motion, they were able to activate global motion detectors.

Contrast of dark and light dots was 100%. For each stimulus and distance, data were collected in 2 sessions of 4 blocks, each composed of 100 trials. For every condition and subject, a cumulative maximum likelihood fit was performed off-line with data obtained in all sessions, based on a Weibull (1951) psychometric function. Thresholds were defined as the coherence level yielding 75% correct discrimination. Student's *t*-tests with significance level of 0.05 were used to compare measured thresholds.

Results and discussion

Figure 2A shows psychometric curves as a function of coherence for anti-Glass stimuli, obtained for different distances between dots within the pair. The horizontal line drawn at chance level separates perception in the direction of white dot (probabilities 0.5–1) from perception in the direction of black dot (probabilities 0–0.5). All subjects perceived a clear direction of motion for distances between $0.4°$ and $0.7°$. In this range, all psychometric curves lie in the upper half of probability range, meaning that motion was always perceived in the direction from the black to the white dot (see Figure 1B). For all subjects, the best performance was obtained for $0.4°$ separation, corresponding to a coherence threshold of 63%. This

separation has been used for anti-Glass patterns in all other experiments in this paper.

Black curves in Figure 2B represent probability of response in the direction of the white dot as a function of coherence, for different displacements of contrast-reversing moving dots corresponding to different speeds. All subjects perceived motion in the direction of the dot presented first (white dot, see also Figure 1C), in accord to the reverse-phi motion illusion (Anstis, 1970). The red curve is the performance obtained with anti-Glass patterns with $0.4°$ separation. The best match to the anti-Glass curve was obtained for the same experimental conditions ($0.4°$, squares). Both stimuli yielded perception of motion in the direction of the white dot with very similar psychometric curves and comparable coherence thresholds: anti-Glass = $(63 \pm 7\%)$, reverse-phi motion = $(63 \pm 11\%)$ ($p = 0.82$). In the rest of the study, we will use this reversing-contrast stimulus.

Green curves in Figure 2C represent probability of responses in the physical direction of motion as a function of coherence, for different displacements of same-polarity moving dots. The best match with the anti-Glass curve (replotted in red) was obtained for $0.1°$ (triangles); coherence thresholds of these two conditions were not significantly different: anti-Glass = $(63 \pm 7\%)$ and regular motion = $(48 \pm 11\%)$ ($p = 0.35$). The curve obtained for the same displacement ($0.4°$, circles) was very far from the anti-Glass curve: anti-Glass = $(63 \pm 7\%)$ and regular motion = $(29 \pm 3\%)$ ($p = 0.015$). This shows that perception of regular motion is stronger than anti-Glass or reverse-phi motion in the same conditions, although it is still possible to find experimental conditions that yield comparable performances. We will use this condition for same-polarity moving dots in the rest of the paper.

The translation of distances into speeds, necessary to compare our results with others, is not straightforward because spatiotemporal properties of our reverse-phi, real motion, and anti-Glass stimuli are quite different; therefore, a common definition of velocity is not obvious. The integration time during the computation of speed for anti-Glass is uniquely determined by the 3- to 5-ms delay (Δt) found between processing of black and white dots (Del Viva et al., 2006). Under this assumption, the velocity $v = \Delta x/\Delta t$ of optimal stimuli is $0.4°/\Delta t > 80°/s$. In our moving stimuli, $\Delta t = 0$, and such an abrupt displacement (Dirac delta) generates a broad spectrum of velocities activating simultaneously many detectors, tuned also to very high speeds, so we need to make a reasonable assumption about integration time. Since the delay between the onset of the first and the second dot is 15 ms, and this is shorter than typical integration times, we assume $\Delta t = 15$ ms, which should correspond to the lag between peak activation of the neural units responding to the two-frame stimulus, whatever the time course of the response. Under this assumption, reverse-phi that best matches anti-Glass move at $\approx 27°/s$ ($\Delta x = 0.4°$), and best-matched motion stimulus has a velocity of $\approx 7°/s$ ($\Delta x = 0.1°$).
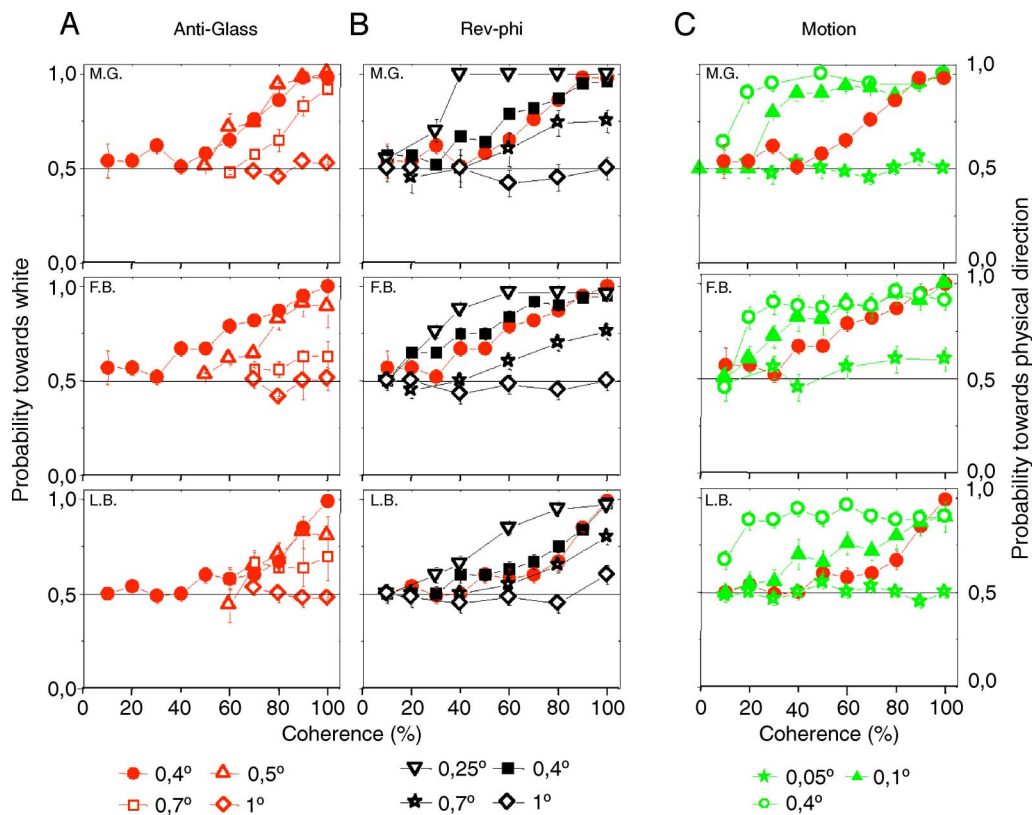
Figure 2. Spatiotemporal properties of stimuli. (A) Probability of motion discrimination in the direction of the white dot as a function of coherence of anti-Glass. Different red symbols represent different distances between dots in the pair. (B) Probability of motion discrimination in the direction of the white dot as a function of coherence of reversing-contrast moving dots (reverse-phi motion). (C) Probability of motion discrimination in the physical direction as a function of coherence of same-polarity moving dots. Different green and black symbols represent different displacements for same-polarity and reverse-phi motion. The red curve replot anti-Glass data in panel A. The horizontal line indicates chance level.

The results presented above show that dynamic anti-Glass patterns give rise to perception of motion in the direction of black to white, for a wide range of distances.

Assuming the definition of velocity given above, the estimated speed range of anti-Glass motion is from 80°/s to 140°/s. In this range, motion from anti-Glass is always perceived in the direction of dots that are processed faster, even though presented simultaneously, consistent with "reverse-phi motion" (Anstis, 1970).

Under our conditions, coherence sensitivities (defined as 1/threshold) for anti-Glass (1.6) matching reversing-contrast (1.66) and regular optic flow (2) were quite low in comparison with those found for regular optic flow (10) (Burr & Santoro, 2001; Morrone et al., 1995). This discrepancy may be due to substantial differences between stimuli: lower speed (7°/s in our stimuli vs. 13°/s in theirs), lower density (0.25/cm² in our stimuli vs. 2.5–5/cm² in theirs), and dot life-time (30 ms in our stimuli vs. 200 ms in theirs).

The maximum displacement allowing perception of reverse-phi motion (0.4°) is also larger than the previously found 0.17° (Sato, 1989), but again very different

experimental conditions and stimuli (such as pattern duration, dot size and number, stimulus size, etc.) can account for the discrepancy.

Contrast thresholds

Stimuli and procedures

We measured motion direction discrimination as a function of Michelson contrast, in 100% coherent anti-Glass patterns, reversing-contrast, and regular moving dots, with the same spatiotemporal characteristics of the first experiment.

Contrast was varied from trial to trial with the method of *constant stimuli*. Subjects indicated the direction of perceived motion, in a two-alternative forced-choice procedure (2AFC) with a single temporal presentation. For each experimental condition, data were collected in 2 sessions of 4 blocks, each composed of 100 trials and all data were fitted (maximum likelihood fit) using a Weibull (1951) psychometric function. Thresholds were defined as

the contrast level yielding 75% correct discrimination. Luminance of light and dark dots corresponding to Michelson contrast 7%, 9%, 13%, and 17% were 65 and 56, 67 and 55, 69 and 51, and 73 and 48 cd/m^2, respectively. Student's *t*-tests with significance level of 0.05 were used to compare thresholds.

Results and discussion

Figure 3A shows the probability of observing motion in the direction of the light dot as a function of Michelson contrast, for both reverse-phi motion and anti-Glass (black and red curves, respectively). The two stimuli yield very similar results, with motion perception becoming less pronounced with decreasing contrast, but always in the direction of the lighter dot. Even at contrasts as low as 13%, more than 75% of presentations were perceived to move toward the lighter dots. Direction

discrimination thresholds for the two stimuli were not statistically different (anti-Glass = (11.9 ± 1.2%), reverse-phi motion = (11.4 ± 1.0%), *p* = 0.76) and so were detection thresholds (anti-Glass = (4.2 ± 0.6%), reverse-phi motion = (4.1 ± 0.6%), *p* = 0.92), shown by arrows.

Figure 3B shows the probability of observing motion in the physical direction as a function of Michelson contrast for both same-polarity motion and anti-Glass (green and red curves, respectively, already shown in Figure 3A). The curves overlap, implying a motion perception with similar contrast dependence for the two stimuli. Direction discrimination thresholds (anti-Glass = (11.9 ± 1.2%), regular motion = (8.7 ± 1.6%), *p* = 0.18) and detection thresholds (shown by arrows) (anti-Glass = (4.2 ± 0.6%), regular motion = (4.0 ± 0.1%), *p* = 0.52) were not statistically different.

Overall, contrasts thresholds of reverse-phi and regular motion are comparable and the latter are in agreement with those found in optic flow (Burr & Santoro, 2001; Morrone et al., 1995).
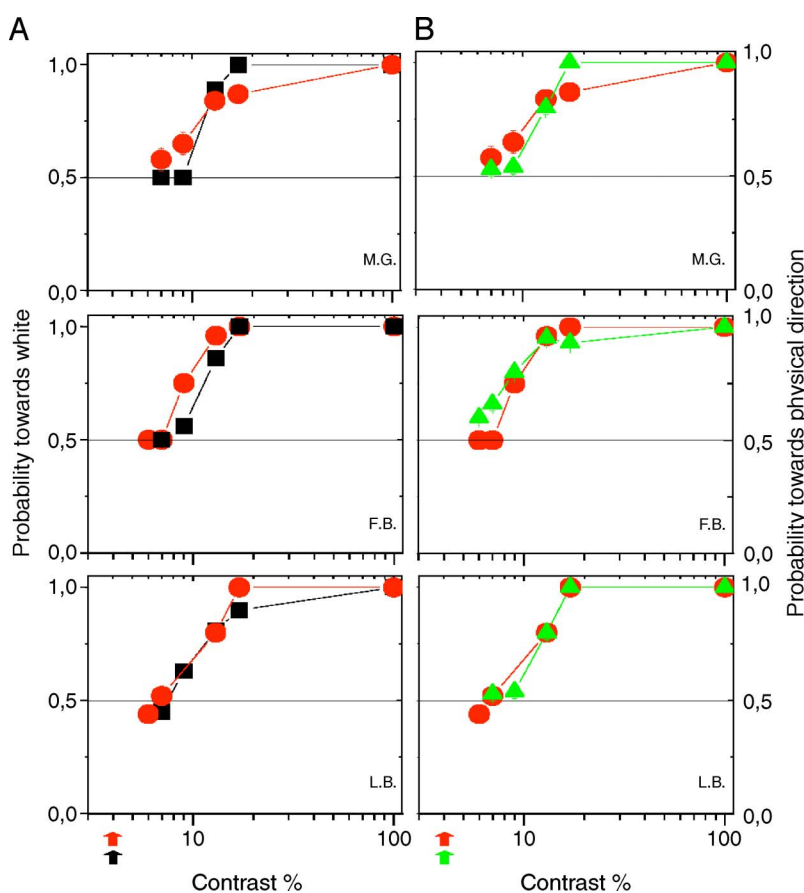

Figure 3. Contrast dependency of stimuli. (A) Probability of motion discrimination in the direction of the white dot as a function of Michelson contrast for anti-Glass patterns (red) and reverse-phi motion (black). Arrows indicate detection thresholds for motion (black) and anti-Glass (red). (B) Probability of motion discrimination in the physical direction as a function of Michelson contrast for same-polarity moving dots (green). The red curve is the same as in panel A. Arrows indicate detection thresholds for motion (green) and anti-Glass (red). Coherence of all stimuli was 100%. The horizontal line indicates chance level.

Annulling motion with anti-Glass patterns

The consistency between speed and contrast dependence of anti-Glass and real motion raises the possibility of processing by a common directional motion mechanism. To test this hypothesis, we presented real motion stimuli and anti-Glass patterns simultaneously in the same display, trying to annul the motion induced by anti-Glass patterns with reversing-contrast or same-contrast moving dots, perceived as moving in the opposite direction. We studied the perception of the resulting motion as a function of the relative strength of the two stimuli, determined by the proportion of dots of each stimulus and their contrast

Stimuli and procedures

Stimuli were combinations of moving dots, either reversing-contrast or same contrast, with anti-Glass patterns. All stimuli had the same spatiotemporal characteristics found in the first experiment. All dots moved coherently along circular trajectories around the screen center, and all anti-Glass pairs were oriented tangentially, so that we always had coherent circular motion. The relative position of light and dark dots was such that anti-Glass motion was perceived in the direction opposite to real motion. Given that dots in anti-Glass were presented simultaneously, moving dots in each single frame were half of the number of anti-Glass dots. The number of moving and anti-Glass dots was thus paired in two frames.

First, we measured motion direction discrimination for this combined stimulus by varying the proportion of anti-Glass pairs with respect to moving dots, keeping constant the total number of dots. For example, we could have 80% moving dots (56×2 frames) and 20% anti-Glass pairs (14 dipoles). The proportion of moving dots, and consequently of anti-pairs, was varied from trial to trial according to the method of *constant stimuli,* randomizing all conditions. The subject's task was to indicate the direction of perceived motion, in a two-alternative forced-choice procedure (2AFC) with a single temporal presentation. In this measurement, contrast of anti-Glass and moving stimuli were 100%.

Then, we repeated the above measurement by setting different contrast values for motion and anti-Glass. Since Michelson contrast yielding chance level was different for our subjects (see Figure 3), some conditions were different between observers (see caption of Figure 4). Luminance of light and dark dots were 80 and 40 cd/m^2 for 30% contrast and 68 and 53 cd/m^2 for 10% contrast (for other values, see the previous section). For each experimental condition, data were collected from each subject in 2 sessions of 5 blocks, each composed of 200 trials. For each subject, the proportion of moving dots matching

anti-Glass (annulling point) was measured by a maximum likelihood fit to an *erf* function, performed off-line with the data obtained in all sessions.

Results and discussion

Figure 4A shows the probability to perceive motion in the direction of reverse-phi (left ordinate) as a function of fraction of reversing-contrast moving dots. The same curves, if read in the opposite direction, represent the probability to perceive motion in the direction of anti-Glass (right ordinate) as a function of fraction of anti-pairs (upper abscissa) because the sum of moving dots and anti-Glass pairs was kept constant. When reversing-contrast and anti-Glass dots had the same contrast (100%, green triangles), perception of motion shifted gradually from one direction to the other when varying the proportion of dots in each stimulus. When the number of dots was equal, subjects could not tell the direction of motion: the mean annulling point, averaged over subjects, was (49.9 ± 1%). In this condition, subjects reported a percept of random noise without motion in either direction. Psychometric curves were symmetrical end-to-end, indicating that similar quantities of anti-Glass and moving dots produced the same amount of motion percept.

In further measurements, we lowered the contrast of reverse-phi stimuli (squares); in this case, a higher number of moving dots were needed to perceive motion in their direction. The same applied to anti-pairs (circles).

In other words, an increase in the proportion of dots can compensate for the lower contrast of a given stimulus down to levels close to the discrimination thresholds (13% for F.B. and L.B.; 10% for M.G.). The psychometric curves are symmetrical when the parameters of the two stimuli are swapped, indicating complete equivalence.

In experiments performed with same-polarity moving dots and anti-Glass patterns with 100% contrast (Figure 4B, green triangles), perception of motion was annulled when the fraction of moving dots was (19 ± 4%). Again, in the annulling condition, the subjects reported a perception of dots moving in random directions. The results indicate that real motion prevails on anti-Glass motion. As in the previous experiment, the strength of each stimulus could be modulated by varying its contrast.

Anti-Glass patterns can annul perception of real motion in the opposite direction, indicating that these two stimuli are processed by the same directional mechanism. However, anti-Glass patterns and contrast-reversing dots give rise to identical perception of motion while same-polarity moving dots are more effective than anti-Glass. The lack of a perception of transparency in the annulling conditions is in agreement with the results of studies performed with real motion stimuli in opposite directions (Qian & Andersen, 1994). In our experiment, the vertical displacement between opposing random dots fields (about 0.1°) and the distances covered during motion (0.4° anti-Glass
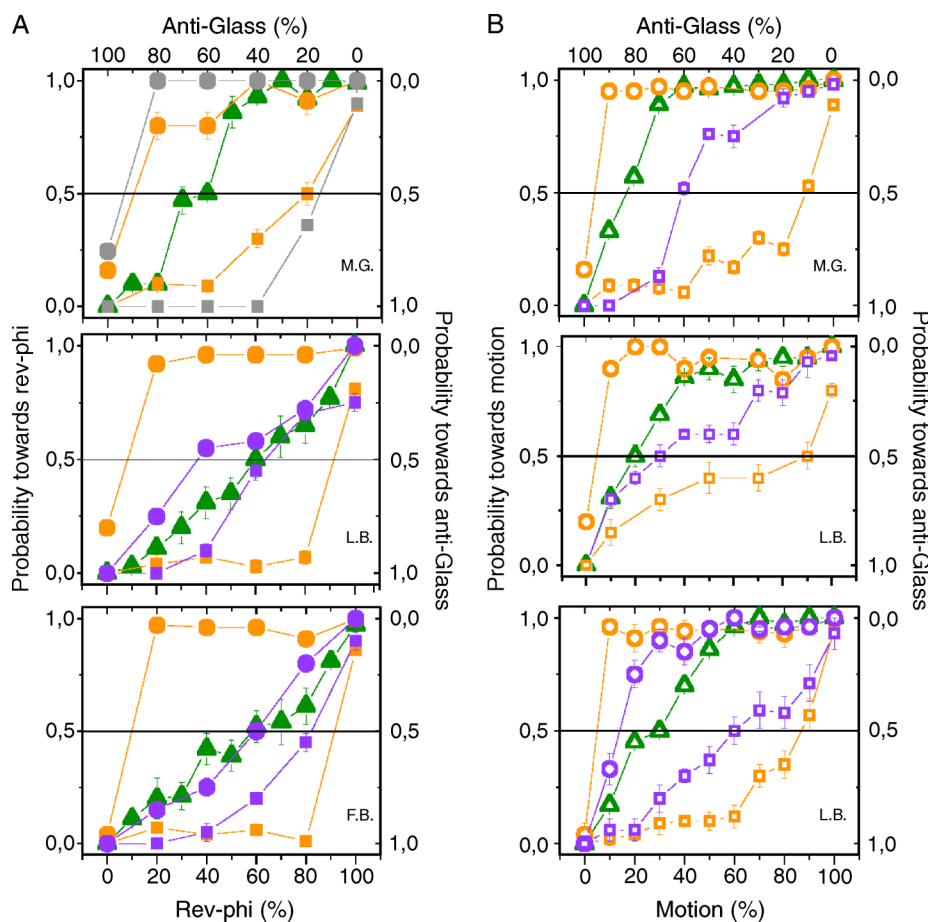
Figure 4. (A) Anti-Glass against reverse-phi motion. Curves represent either the probability of motion discrimination in the direction of reverse-phi (left ordinate) as a function of fraction of moving dots (lower abscissa), or the probability of motion discrimination in the direction of anti-Glass (right ordinate) as a function of fraction of anti-Glass pairs (upper abscissa). The number of anti-Glass plus moving dots is constant: ▲, contrast anti-Glass and reverse-phi = 100%; ●, contrast anti-Glass = 30%, contrast reverse-phi = 100%; ●, contrast anti-Glass = 13%, contrast reverse-phi = 100%; ●, contrast anti-Glass = 10%, contrast reverse-phi = 100%; ■, contrast anti-Glass = 100%, contrast reverse-phi = 30%; ■, contrast anti-Glass = 100%, contrast reverse-phi = 13%; ■, contrast anti-Glass = 100%, contrast reverse-phi = 10%. (B) Anti-Glass against motion. Motion discrimination in the direction of moving dots (left ordinate)—or anti-Glass (right ordinate)—as a function of fraction of moving dots (lower abscissa)—or anti-pairs (upper abscissa). The number of anti-Glass plus moving dots is constant. ▲, contrast anti-Glass and motion = 100%; ○, contrast anti-Glass = 30%, contrast motion = 100%; ○, contrast anti-Glass = 13%, contrast motion = 100%; □, contrast anti-Glass = 100%, contrast motion = 30%; □, contrast anti-Glass = 100%, contrast motion = 13%.

and reverse-phi; 0.1° motion) are in agreement with corresponding values (less than 0.12° and 0.4°, respectively) reported by Qian and Andersen (1994) in order to expect integration rather than transparency.

Contrast dependency of the annulment point suggests that the common mechanism could be located at low level in the visual system, as it is known that perceived local motion is more dependent on contrast than perceived global motion (Morrone et al., 1995; Shiori, Ito, Sakurai, & Yaguchi, 2002), and that MT neurons are less effective in signaling absolute levels of contrast than LGN or V1 neurons (Sclar, Maunsell, & Lennie, 1990). To further test the interactions between stimuli as a function of contrast, we performed a sub-threshold summation experiment.

Sub-threshold summation

Stimuli and procedure

Stimuli were anti-Glass pairs superimposed on moving dots, either reversing-contrast or same contrast. The relative position of light and dark dots was such that anti-Glass motion and real motion were expected to be perceived in the same direction. Spatiotemporal characteristics of stimuli were those found in the first experiment, and their coherence was 100%. The number of moving and anti-Glass dots was paired in two frames as in previous experiments. We measured direction discrimination

thresholds by varying simultaneously the contrast of anti-Glass and motion stimuli of the same amount (i.e., 7% and 7%, etc.). Contrast was varied from trial to trial according to a QUEST staircase procedure (Watson & Pelli, 1983). For each condition, data were collected in 2 sessions of 3 blocks, each composed of 200 trials, and all data were fitted (maximum likelihood fit) with a Weibull (1951) psychometric function. Thresholds were defined as the contrast level yielding 75% correct discrimination. Student's *t*-tests with significance level of 0.05 were used to compare mean thresholds.

Results and discussion

Red-filled circles in Figure 5 represent the probability of perceiving motion in the direction of the white dot as a function of contrast of anti-Glass, obtained with 70 anti-Glass pairs presented alone (same data of Figure 3). The blue curve, obtained by adding 70 contrast-reversing moving dots to the 70 anti-pairs, is shifted leftward: thresholds shift from (11.9 ± 1.2%) to (7.8 ± 0.3%) ($p = 0.019$). This indicates that motion is perceived at contrasts well below the individual thresholds for anti-Glass or motion.

Following Meese and Harris (2001), we employed the Minkowsky metric to evaluate the degree of summation in our experiment

$$\nu_{\text{compound}} = \left(\nu_{\text{stimA}}^{k} + \nu_{\text{stimB}}^{k} \right)^{\frac{1}{k}}, \qquad (1)$$

where ν_{compound} is the sensitivity for the compound stimulus (anti-Glass + reverse-phi motion) and ν_{stimA} and ν_{stimB} are the sensitivities of individual stimuli. The exponent k is the degree of summation: $k = 1$ for linear summation, $k = 2$ for quadratic summation, and $k = 3$ to 4 for probability summation between independent mechanisms (Graham, 1989). For our experiment, we found $k = 1.67 \pm 0.24$, indicating a sub-threshold summation intermediate between linear and quadratic, excluding probability summation between independent channels.

The curve for real motion plus anti-Glass (cyan curve) is also shifted significantly toward left: thresholds shift from (11.9 ± 1.2%) to (5.8 ± 0.6%) ($p = 0.009$). In this case, we obtain $k = 1.27 \pm 0.08$, again indicating sub-threshold summation intermediate between linear and quadratic.

As a control, we measured contrast thresholds from 140 anti-Glass pair (hollow circles) and compared with thresholds obtained with 70 pairs (thresholds shift from (11.9 ± 1.2%) to (7 ± 0.5%), $p = 0.015$). The results are indistinguishable from those obtained with motion plus anti-Glass (reverse-phi + anti-Glass: $p = 0.24$; regular motion + anti-Glass: $p = 0.23$), thus showing that the sub-threshold summation happens in exactly the same way between different and same stimuli.

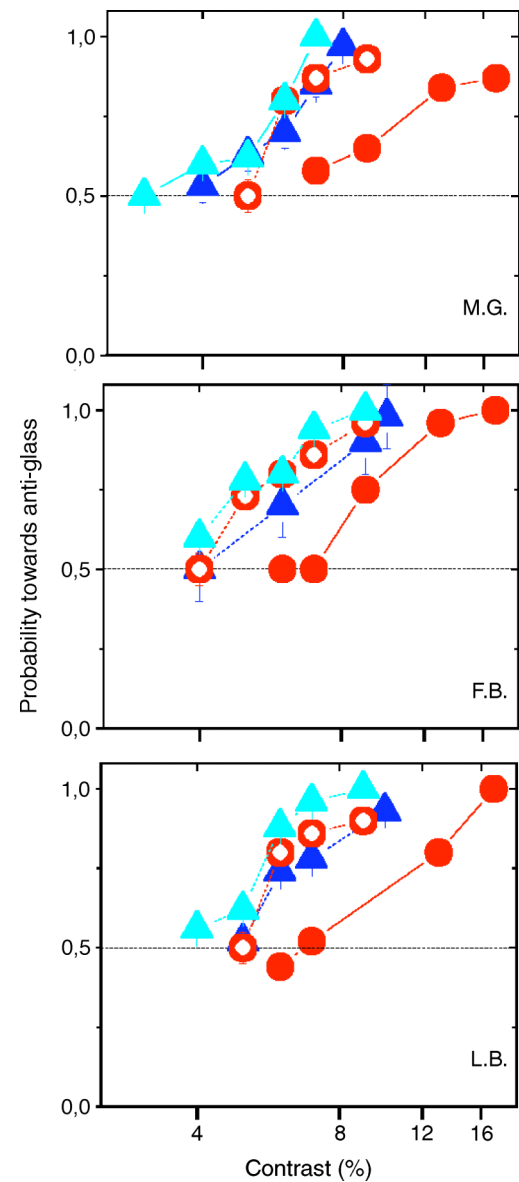These facts demonstrate that there must be a neural motion mechanism where the two stimuli are added

Figure 5. Sub-threshold summation. Probability of motion discrimination in the direction of anti-Glass (toward white dot) as a function of contrast of anti-Glass. Red filled circles: stimulus composed by 70 anti-Glass pairs (also shown in Figure 3). Blue: stimulus composed by 70 anti-Glass pairs and 70 reversing-contrast moving dots. Cyan: stimulus composed by 70 anti-Glass pairs and 70 same-polarity moving dots. Red hollow circles: stimulus composed by 140 anti-Glass pairs.

together in an almost-linear way before a thresholding effect occurs.

Local motion

Although the annulling and the sub-threshold summation experiments do not rule out the possibility of two

different populations of local motion detectors, they show that if there are two such populations, their outputs are integrated in a global motion perception. The fact that the global integration is so good strongly suggests, but does not prove, that the same type of local motion detector is responsible for reporting a motion signal for both anti-Glass and real motion. If these stimuli at local level had similar properties, this could constitute further evidence in favor of low-level motion mechanisms of the same type.

We investigated this issue by measuring motion direction discrimination as a function of displacement and as a function of contrast of a single moving dot, a single contrast reversing dot, an anti-Glass pair, a Glass pair.

Stimuli and procedure

Dots were positioned in the center of the screen, each subtending 0.3° of visual angle.

Moving and reversing-contrast dots

Direction of motion could be either leftward or rightward, randomized between trials. We presented two-frame motion, each frame lasting 15 ms, for a total duration of 30 ms. Direction discrimination was measured as a function of displacement (from 0.4° to 1.25°), and during this measurement, the dot contrast was kept constant (100%). Direction discrimination was measured also as function of contrast (from 5% to 30%). During this measurement, displacement was kept constant (0.4°).

Glass and anti-Glass

The dipole was oriented horizontally, and the relative position of black and white dots in anti-Glass was randomized between trials. Total duration of the stimulus was 30 ms. Direction discrimination was measured as a function of displacement (from 0.4° to 1.25°), and during this measurement, dot contrast was kept constant (100%). Direction discrimination was measured also as function of contrast (from 5% to 30%). During this measurement displacement was kept constant (0.4°).

In both measurements, dot displacement and contrast were varied from trial to trial according to the method of *constant stimuli,* randomizing all conditions. The subject's task was to indicate the direction of perceived motion, in a two-alternative forced-choice procedure (2AFC) with a single temporal presentation. Correct direction was defined as

1. physical direction for regular motion;
2. opposite to physical direction for reverse-phi;
3. toward white dot for anti-Glass; and
4. toward left for Glass.

We ran 100 trials for each subject for each condition. Two of the previous subjects participated to all experiments. Two other naive subjects (N.G. and B.P.) discriminated the direction of local motion only for a displacement of 0.4°.

Results and discussion

The upper part of Figure 6A shows the probability of perceiving the correct direction of motion for all stimuli, for a displacement of 0.4°, which is optimal for anti-Glass (see Experiment 1). All subjects detected equally well motion direction of all stimuli, except the Glass pair where, as expected, direction was ambiguous.

All local stimuli yielded very similar direction discrimination, also when displacement was varied in the whole interval used in global motion tests, as shown in lower panels of Figure 6A, dropping dramatically beyond 0.7°. Results for Glass are not shown because they always gave 50% correct discrimination.

This experiment demonstrates that detection of local motion of dots and anti-Glass is perfectly equivalent when varying their spatial displacement. From this experiment, it is also possible to figure out a lower limit for spatial frequency tuning of detectors for local anti-Glass and real motion: The maximum value is obtained for 0.4° displacement for all stimuli, which correspond to a spatial frequency 2.5 cycles/deg, the lowest detectable in this experiment.

Figure 6B shows the probability of perceiving correct direction of motion for all stimuli, for a displacement of 0.4°, as a function of contrast. All psychometric curves overlap perfectly, meaning that contrast sensitivity of local motion system is the same for all three stimuli presented here. Mean direction thresholds, defined as 75% of psychometric functions, are (12.3 ± 0.7%) for anti-Glass, (12.5 ± 0.9%) for reversing-contrast motion, and (11.2 ± 0.6%) for regular motion. These values are not much higher than those found for the global stimuli.

General discussion

Glass and anti-Glass patterns are ideal stimuli to investigate properties of local and global integration mechanisms as well as form and motion processing. Results presented in this paper help to elucidate the relationships between these two stimuli.

The goal of this paper is to study the motion illusion induced by anti-Glass patterns, and we have shown that perception of global motion induced by anti-Glass patterns is comparable to that obtained with real motion, either contrast-reversing or not, indicating that anti-Glass patterns stimulate the same directional motion mechanisms. We also found that a single moving point, either contrast-reversing or not, elicits comparable motion perception to an anti-Glass pair if motion is matched for
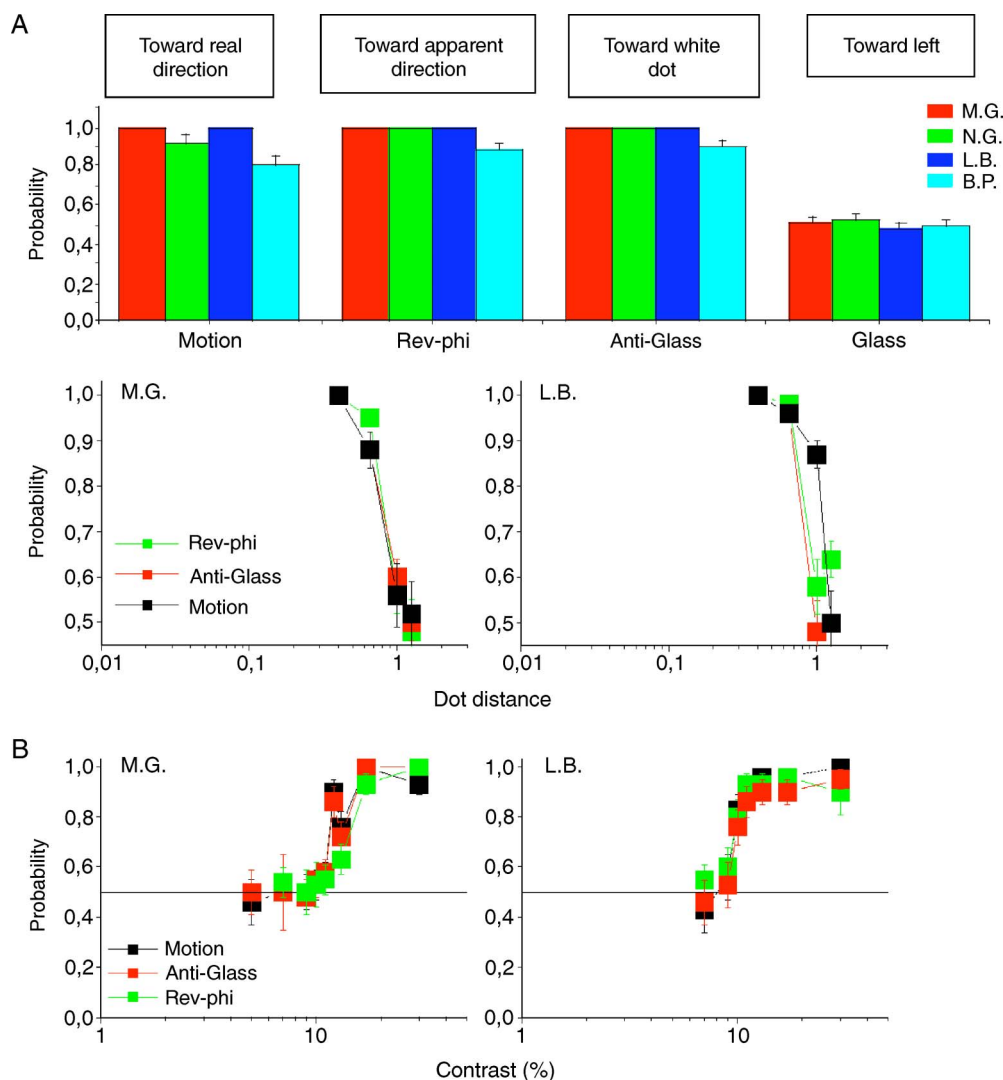
Figure 6. Local motion with different stimuli. (A) Upper panels. From left: motion direction discrimination (probability of correct responses) for dot distance of 0.4° of four subjects for a single moving dot, a single contrast reversing moving dot, one anti-Glass pair, one Glass pair. Definition of correct response (labels above graphs) depends on the kind of stimulus. Lower panels. Motion direction discrimination as a function of distance for one moving dot, one contrast reversing moving dot, one anti-Glass pair (two subjects). Contrast was 100%. (B) Motion direction discrimination as a function of contrast for one moving dot, one contrast reversing moving dot, one anti-Glass pair (two subjects). Dot distance was 0.4°. Definition of correct response is the same as in panel A.

duration and distance. The close similarities observed at local level between these two types of motion and the contrast dependency of global motion perception strongly suggest that the two kind of motions are encoded at low levels by the same type of motion system (Morrone et al., 1995; Sclar et al., 1990), rather than by local different mechanisms combined at a higher level by a non-selective motion detector (Albright, 1992).

Overall, we can conclude that, at least in the spatio-temporal range explored here, anti-Glass are treated by the human visual system in the same way as real motion and reverse-phi stimuli. In particular, anti-Glass and reverse-phi motion are perceived in the direction opposite to the temporal processing of dots, thus proving to be two special cases of the same phenomenon. The powerful

motion experience generated by really moving objects cannot be equated to the perception of this illusion that is perceived for short time intervals that probably never occur in natural situations. From the results of our experiments, we conjecture that there exist a set of local motion detectors tuned to these spatiotemporal parameters that process all stimuli, illusory or not. In addition to these detectors, there are many others tuned to a broader range of speed values, triggered by slower motion or by objects moving over larger areas, that we experience in everyday life. In this respect, anti-Glass motion is real motion, but not all real motion is equivalent to anti-Glass motion perception.

Overall, perception of form and apparent motion in Glass and anti-Glass patterns could be described within a general

Del Viva & Gori

framework of visual networks (Van Essen, 1995; Van Essen, Anderson, & Felleman, 1992) that hypothesize a hierarchical analysis of form and motion, realized in two stages. In an early stage, visual features are analyzed in parallel by local orientation units (Hubel & Wiesel, 1962; Hubel & Wiesel, 1977) and local motion detectors with a preferred motion direction (Movshon, Adelson, Gizzi, & Newsome, 1985; Hubel, 1989; Tovèe, 1994), widely found in early visual areas. The output from local orientation mechanisms is integrated at a higher level by neurons with larger receptive fields, responsible for perception of complex structures located, for example, in visual areas V4 or IT (Tanaka, 1992; Wilkinson et al., 2000). Similarly, outputs from motion detectors selective to specific directions are integrated by neurons with larger receptive fields located in global motion areas such as MT, MSTd, or STS (Britten & van Wezel, 1998; Duffy & Wurtz, 1991; Mikami et al., 1986a; 1986b; Movshon et al., 1985; Tanaka et al., 1989).

Different perceptions elicited by Glass and anti-Glass patterns can thus be explained by a substantial difference of neural structures involved in the initial stage of analysis. Glass patterns could undergo initial local form integration along dipoles due to local orientation detectors, performed by early visual areas such as V1 or V2 (Movshon et al., 2003; Smith et al., 2002). This initial stage could be followed by global form integration (Wilkinson et al., 2000) and integration along flow trajectories performed by global motion areas (Krekelberg et al., 2003).

Anti-Glass patterns are not expected to elicit local form perception in early visual areas: Mean activation of local orientation units should be null if two identical dots with opposite luminance are presented simultaneously in their receptive field (Glass & Switkes, 1976). Some evidence showing there is no difference between detection of circular anti-Glass and random oriented pairs also demonstrates scarce involvement of global form areas (Wilson, Switkes, & De Valois, 2004).

On the other hand, results presented in this study strongly suggest the involvement of low-level contrast-dependent local motion detectors that can be modelled by Reichardt (1961) detectors, possibly localized in early visual areas such as V1 or V2 (Hubel, 1989; Movshon et al., 1985, 2003; Tovèe, 1994) (see Figure 7). The input to these motion detectors could be provided by sub-cortical neurons, where a temporal delay in the processing of the dark dots is generated, maybe due to differential temporal processing between the primate on and off systems (Chichilnisky & Kalmar, 2002; Ueno et al., 2004) (Figure 7). Anti-Glass patterns appear to move in the direction opposite to the temporal processing of dots, like reverse-phi motion stimuli (Anstis, 1970), and produce the same motion perception of reverse-phi. Recordings from direction-selective cells in monkey V1 (Conway & Livingstone, 2003), as well as correlation of motion energy models (Adelson & Bergen, 1985) and Reichardt models (van Santen & Sperling, 1985), can account for motion and reverse-phi motion, even though it is still
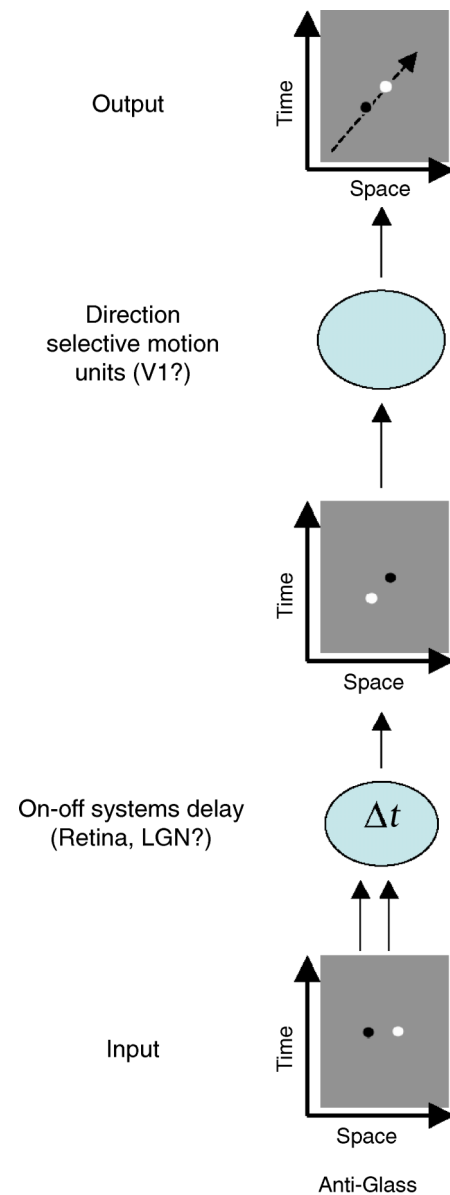

Figure 7. Descriptive model of motion generated by anti-Glass patterns. Dots in the anti-Glass pairs are presented simultaneously to the visual system. A sub-cortical delay (~3 ms) between on and off pathways causes a latency in the processing of the dark dot with respect to the white. This latency can generate a motion signal in cortical direction-selective neurons, indistinguishable from that elicited by contrast-reversing real motion. The vector sign of velocity is inverted like in reverse-phi motion.

unclear how neurons accomplish this. These low-level local motion detectors could extract direction of motion of anti-Glass patterns before it is integrated along complex motion trajectories in global motion areas (Heeger et al., 1999; Qian & Andersen, 1994).

Glass pattern sequences made of dots with same-polarity (i.e., Ross et al., 2000) are not expected to stimulate these directional detectors because there cannot be a delay between dots with same luminance. This could

be the reason why they produce perception of motion without any sense of direction. The question regarding how same-polarity Glass patterns produce global sense of motion without producing local or global direction is beyond the scope of this work. In fact, our experiments lead to think that the mechanisms causing motion perception in anti-Glass stimuli are very different from those responsible for motion perception in Glass stimuli. For the latter, dipoles could be interpreted by the visual system as *motion streaks* (Geisler, 1999) and therefore could be sufficient to trigger motion perception. An alternative explanation could rely on the existence of connections between global form and global motion integration areas (Kourtzi & Kanwisher, 2000; Krekelberg et al., 2003; Van Essen, 1995) that might guarantee unity of perception and provide a system able to cope with complex environments with multiple objects in motion.

Acknowledgments

References

Adelson, E. H., & Bergen, J. R. (1985). Spatiotemporal energy models for the perception of motion. *Journal of the Optical Society of America A, Optics and Image Science, 2,* 284–299. [PubMed]

Albright, T. D. (1992). Form-cue invariant motion processing in primate visual cortex. *Science, 255,* 1141–1143. [PubMed]

Anstis, S. M. (1970). Phi movement as a subtraction process. *Vision Research, 10,* 1411–1430. [PubMed]

Backus, B. B., & Oruç, I. (2006). Illusory motion from change over time in the response to contrast and luminance. *Journal of Vision, 5*(11):10, 1055–1069, http://journalofvision.org/5/11/10, doi:10.1167/5.11.10. [PubMed] [Article]

Barlow, H. B., & Olshausen, B. A. (2004). Convergent evidence for the visual analysis of optic flow through anisotropic attenuation of high spatial frequencies. *Journal of Vision, 4*(6):1, 415–426, http://journalofvision.org/4/6/1/, doi:10.1167/4.6.1. [PubMed] [Article]

Britten, K. H., & van Wezel, R. J. (1998). Electrical microstimulation of cortical area MST biases heading perception in monkeys. *Nature Neuroscience, 1,* 59–63. [PubMed] [Article]

Brooks, A., van der Zwan, R., & Holden, J. (2003). An illusion of coherent global motion arising from single brief presentations of a stationary stimulus. *Vision Research, 43,* 2387–2392. [PubMed]

Burr, D., & Ross, J. (2006). The effects of opposite-polarity dipoles on the detection of Glass patterns. *Vision Research, 46,* 1139–1144. [PubMed]

Burr, D. C., & Santoro, L. (2001). Temporal integration of optic flow, measured by contrast and coherence thresholds. *Vision Research, 41,* 1891–1899. [PubMed]

Cardinal, K. S., & Kiper, D. C. (2003). The detection of colored Glass patterns. *Journal of Vision 3*(3):2, 199–208, http://journalofvision.org/3/3/2/, doi:10.1167/3.3.2. [PubMed] [Article]

Chichilnisky, E. J., & Kalmar, R. S. (2002). Functional asymmetries in ON and OFF ganglion cells of primate retina. *Journal of Neuroscience, 22,* 2737–2747. [PubMed] [Article]

Conway, B. R., Kitaoka, A., Yazdanbakhsh, A., Pack, C. C., & Livingstone, M. S. (2005). Neural basis for a powerful static motion illusion. *Journal of Neuroscience, 25,* 5651–5656. [PubMed] [Article]

Conway, B. R., & Livingstone, M. S. (2003). Space-time maps and two-bar interactions of different classes of direction-selective cells in macaque V1. *Journal of Neurophysiology, 89,* 2726–2742. [PubMed] [Article]

Dakin, S. C. (1997). Glass patterns: Some contrast effects are re-evaluated. *Perception, 26,* 253–268. [PubMed]

Dakin, S. C., & Bex, P. J. (2001). Local and global visual grouping: Tuning for spatial frequency and contrast. *Journal of Vision, 1*(2):4, 99–111, http://journalofvision.org/1/2/4/, doi:10.1167/1.2.4. [PubMed] [Article]

Del Viva, M. M., Gori, M., & Burr, D. C. (2006). Powerful motion illusion caused by temporal asymmetries in ON and OFF visual pathways. *Journal of Neurophysiology, 95,* 3928–3932. [PubMed] [Article]

Duffy, C. J., & Wurtz, R. H. (1991). Sensitivity of MST neurons to optic flow stimuli: I. A continuum of response selectivity to large-field stimuli. *Journal of Neurophysiology, 65,* 1329–1345. [PubMed]

Geisler, W. S. (1999). Motion streaks provide a spatial code for motion direction. *Nature, 400,* 65–69. [PubMed]

Glass, L. (1969). Moire effect from random dots. *Nature, 223,* 578–580. [PubMed]

Glass, L., & Switkes, E. (1976). Pattern recognition in humans: Correlations which cannot be perceived. *Perception, 5,* 67–72. [PubMed]

Graham (1989). *Visual pattern analyzers.* Oxford: Oxford University Press.

Heeger, D. J., Boynton, G. M., Demb, J. B., Seidemann, E., & Newsome, W. T. (1999). Motion opponency in visual cortex. *Journal of Neuroscience, 19,* 7162–7174. [PubMed] [Article]

Hegdé, J., & Van Essen, D. C. (2000). Selectivity for complex shapes in primate visual area V2. *Journal of Neuroscience, 20,* RC61. [PubMed] [Article]

Hubel, D. H. (1989). *Eye, brain and vision* (vol. 22). New York: Scientific American Library.

Hubel, D. H., & Wiesel, T. N. (1962). Receptive fields, binocular interaction and functional architecture in the cat's visual cortex. *The Journal of Physiology, 160,* 106–154. [PubMed] [Article]

Hubel, D. H., & Wiesel, T. N. (1977). Ferrier lecture. Functional architecture of macaque monkey visual cortex. *Proceedings of the Royal Society of London B: Biological Sciences, 198,* 1–59. [PubMed]

Kourtzi, Z., & Kanwisher, N. (2000). Activation in human MT/MST by static images with implied motion. *Journal of Cognitive Neuroscience, 12,* 48–55. [PubMed]

Krekelberg, B., Dannenberg, S., Hoffmann, K. P., Bremmer, F., & Ross, J. (2003). Neural correlates of implied motion. *Nature, 424,* 674–677. [PubMed]

Krekelberg, B., Vatakis, A., & Kourtzi, Z. (2005). Implied motion from form in the human visual cortex. *Journal of Neurophysiology, 94,* 4373–4386. [PubMed] [Article]

Kurki, I., Laurinen, P., Peromaa, T., & Saarinen, J. (2003). Spatial integration in Glass patterns. *Perception, 32,* 1211–1220. [PubMed]

Meese, T. S., & Harris, M. G. (2001). Independent detectors for expansion and rotation, and for orthogonal components of deformation. *Perception, 30,* 1189–1202. [PubMed]

Mikami, A., Newsome, W. T., & Wurtz, R. H. (1986a). Motion selectivity in macaque visual cortex: I. Mechanisms of direction and speed selectivity in extrastriate area MT. *Journal of Neurophysiology, 55,* 1308–1327. [PubMed]

Mikami, A., Newsome, W. T., & Wurtz, R. H. (1986b). Motion selectivity in macaque visual cortex. II. Spatiotemporal range of directional interactions in MT and V1. *Journal of Neurophysiology, 55,* 1328–1339. [PubMed]

Morrone, M. C., Burr, D. C., & Vaina, L. M. (1995). Two stages of visual processing for radial and circular motion. *Nature, 376,* 507–509. [PubMed]

Morrone, M. C., Tosetti, M., Montanaro, D., Fiorentini, A., Cioni, G., & Burr, D. C. (2000). A cortical area that responds specifically to optic flow, revealed by fMRI. *Nature Neuroscience, 3,* 1322–1328. [PubMed] [Article]

Movshon, J. A., Adelson, E. H., Gizzi, M. S., & Newsome, W. T. (1985). The analysis of moving visual patterns. In C. Chagas, R. Gattass, & C. Gross (Eds.), *Study week on pattern recognition mechanisms* (pp. 117–151). Rome: Vatican Press.

Movshon, J. A., Smith, M. A., & Kohn, A. (2003). Responses to Glass patterns in macaque V1 and V2 [Abstract]. *Journal of Vision, 3*(9):151, 151a, http://journalofvision.org/3/9/151/, doi:10.1167/3.9.151.

Newsome, W. T., & Pare, E. B. (1988). A selective impairment of motion perception following lesions of the middle temporal visual area (MT). *Journal of Neuroscience, 8,* 2201–2211. [PubMed] [Article]

Prazdny, K. (1986). Some new phenomena in the perception of Glass patterns. *Biological Cybernetics, 53,* 153–158. [PubMed]

Qian, N., & Andersen, R. A. (1994). Transparent motion perception as detection of unbalanced motion signals. II. Physiology. *Journal of Neuroscience, 14,* 7367–7380. [PubMed] [Article]

Reichardt, W. (1961). Autocorrelation, a principle for evaluating of sensory information by central nervous system. In W. Rosenblith (Ed.), *Sensory communication* (pp. 303–317). New York: Wiley.

Ross, J. (2004). The perceived direction and speed of global motion in Glass pattern sequences. *Vision Research, 44,* 441–448. [PubMed]

Ross, J., Badcock, D. R., & Hayes, A. (2000). Coherent global motion in the absence of coherent velocity signals. *Current Biology, 10,* 679–682. [PubMed] [Article]

Sato, T. (1989). Reversed apparent motion with random dot patterns. *Vision Research, 29,* 1749–1758. [PubMed]

Sclar, G., Maunsell, J. H., & Lennie, P. (1990). Coding of image contrast in central visual pathways of the macaque monkey. *Vision Research, 30,* 1–10. [PubMed]

Seu, L., & Ferrera, V. P. (2001). Detection thresholds for spiral Glass patterns. *Vision Research, 41,* 3785–3790. [PubMed]

Shioiri, S., Ito, S., Sakurai, K., & Yaguchi, H. (2002). Detection of relative and uniform motion. *Journal of the Optical Society of America A, Optics, Image Science, and Vision, 19,* 2169–2179. [PubMed]

Smith, M. A., Bair, W., & Movshon, J. A. (2002). Signals in macaque striate cortical neurons that support the perception of Glass patterns. *Journal of Neuroscience, 22,* 8334–8345. [PubMed] [Article]

Tanaka, K. (1992). Inferotemporal cortex and higher visual functions. *Current Opinion in Neurobiology, 2,* 502–505. [PubMed]

Tanaka, K., Fukada, Y., & Saito, H. A. (1989). Underlying mechanisms of the response specificity of

expansion/contraction and rotation cells in the dorsal part of the medial superior temporal area of the macaque monkey. *Journal of Neurophysiology, 62,* 642–656. [PubMed]

Tovèe, M. (1994). *An introduction to the visual system.* Cambridge: University Press.

Ueno, S., Kondo, M., Niwa, Y., Terasaki, H., & Miyake, Y. (2004). Luminance dependence of neural components that underlies the primate photopic electroretinogram. *Investigative Ophthalmology & Visual Science, 45,* 1033–1040. [PubMed] [Article]

Van Essen, D. C. (1995). Behind the optic nerve: An inside view of the primate visual system. *Transactions of the American Ophthalmological Society, 93,* 123–133. [PubMed] [Article]

Van Essen, D. C., Anderson, C. H., & Felleman, D. J. (1992). Information processing in the primate visual system: An integrated systems perspective. *Science, 255,* 419–423. [PubMed]

van Santen, J. P., & Sperling, G. (1985). Elaborated Reichardt detectors. *Journal of the Optical Society of America A, Optics and Image Science, 2,* 300–321. [PubMed]

Watson, A. B., & Pelli, D. G. (1983). QUEST: A Bayesian adaptive psychometric method. *Perception & Psychophysics, 33,* 113–120. [PubMed]

Weibull, W. A. (1951). A statistical distribution function of wide applicability. *Journal of Applied Mechanics, 18,* 292–297.

Wilkinson, F., James, T. W., Wilson, H. R., Gati, J. S., Menon, R. S., & Goodale, M. A., et al. (2000). An fMRI study of the selective activation of human extrastriate form vision areas by radial and concentric gratings. *Current Biology, 10,* 1455–1458. [PubMed] [Article]

Wilson, H. R., & Wilkinson, F. (1998). Detection of global structure in Glass patterns: Implications for form vision. *Vision Research, 38,* 2933–2947. [PubMed]

Wilson, H. R., Wilkinson, F., & Asaad, W. (1997). Concentric orientation summation in human form vision. *Vision Research, 37,* 2325–2330. [PubMed]

Wilson, J. A., Switkes, E., & De Valois, R. L. (2004). Glass pattern studies of local and global processing of contrast variations. *Vision Research, 44,* 2629–2641. [PubMed]

Zeki, S., Watson, J. D., & Frackowiak, R. S. (1993). Going beyond the information given: The relation of illusory visual motion to brain activity. *Proceedings of the Royal Society B: Biological Sciences, 252,* 215–222. [PubMed]